Journal of Hazardous Materials 474 (2024) 134592

Contents lists available at ScienceDirect

Journal of Hazardous Materials

journal homepage: www.elsevier.com/locate/jhazmat

Seasonal drives on potentially toxic elements dynamics in a tropical estuary impacted by mine tailings

Amanda Duim Ferreira [a], Owen W. Duckworth [b], Hermano Melo Queiroz [c], Gabriel Nuto Nóbrega [d], Diego Barcellos [e], Ângelo Fraga Bernardino [f], Xosé L. Otero [g], Tiago Osório Ferreira [a,*]

[a] Department of Soil Science, "Luiz de Queiroz" College of Agriculture, University of São Paulo, Piracicaba, SP, Brazil
[b] Department of Crop and Soil Science, North Carolina State University, Raleigh, NC, United States
[c] Department of Geography, University of São Paulo, Av. Prof. Lineu Prestes, 338, Cidade Universitária, 05508–900, São Paulo, SP, Brazil
[d] Departament of Soil Science, Federal University of Ceará, Fortaleza, CE, Brazil
[e] Department of Environmental Sciences. Federal University of São Paulo, São Paulo, SP, Brazil
[f] Grupo de Ecologia Bentônica, Departamento de Oceanografia, Universidade Federal do Espírito Santo, Vitória, ES, Brazil
[g] Departamento de Edafología y Química Agrícola, Facultad de Biología, Universidad de Santiago de Compostela, Spain

HIGHLIGHTS

- Soil clay contents and soil pH were higher during the wet season.
- Higher Fe availability in the estuarine soils during the dry seasons.
- Potential toxic elements bioavailability increased over time.
- Climatic factors explained 48% of PTEs' bioavailability in the estuarine soils.
- Short-range ordered oxides exert control over PTEs' bioavailability.

GRAPHICAL ABSTRACT

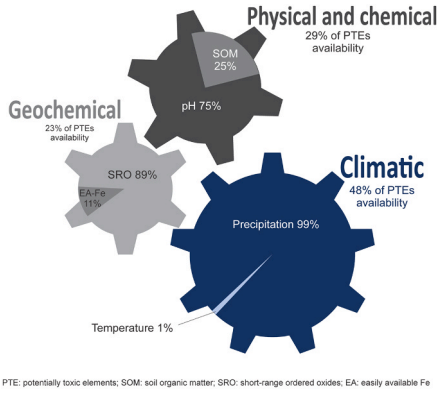

PTE: potentially toxic elements; SOM: soil organic matter; SRO: short-range ordered oxides; EA: easily available Fe

ARTICLE INFO

Keywords:
Seasonal dynamics
PTE fate
PTE bioavailability
Risk modeling

ABSTRACT

This study investigates the impact of seasonality on estuarine soil geochemistry, focusing on redox-sensitive elements, particularly Fe, in a tropical estuary affected by Fe-rich mine tailings. We analyzed soil samples for variations in particle size, pH, redox potential (Eh), and the content of Fe, Mn, Cr, Cu, Ni, and Pb. Additionally, sequential extraction was employed to understand the fate of these elements. Results revealed dynamic changes in the soil geochemical environment, transitioning between near-neutral and suboxic/anoxic conditions in the wet season and slightly acidic to suboxic/oxic conditions in the dry season. During the wet season, fine particle deposition (83%) rich in Fe (50 g kg^{-1}), primarily comprising crystalline Fe oxides, occurred significantly. Conversely, short-range ordered Fe oxides dominated during the dry season. Over consecutive wet/dry seasons,

* Corresponding author.
E-mail address: toferreira@usp.br (T.O. Ferreira).

https://doi.org/10.1016/j.jhazmat.2024.134592
Received 19 December 2023; Received in revised form 9 April 2024; Accepted 10 May 2024
Available online 17 May 2024

substantial losses of Fe (−55%), Mn (−41%), and other potentially toxic elements (Cr: −44%, Cu: −31%, Ni: −25%, Pb: −9%) were observed. Despite lower pseudo-total PTE contents, exchangeable PTEs associated with carbonate content increased over time (Cu: +188%, Ni: +557%, Pb: +99%). Modeling indicated climatic variables and short-range oxides substantially influenced PTE bioavailability, emphasizing the ephemeral Fe oxide control during the wet season and heightened ecological and health risks during the dry seasons.

1. Introduction

Seasonal flooding drives changes in the redox conditions of estuarine soils and sediments [1,2], which influences ecosystem structure and function [3–6]. During the wet season, the combined effects of suspended sediment deposition, increasing dissolved organic carbon content, and freshwater input can promote more reducing conditions, which may affect the dynamics of potentially toxic elements (PTEs) in estuaries [3–6]. Conversely, suboxic to oxic conditions may be established during seasonal droughts, which may also affect the bioavailability of PTEs [7,8]. For example, the low water content in wetland soils during dry periods may favor the oxidation of sulfides, which potentially releases PTEs [7,8]; these conditions may promote the formation of short-range Fe and Mn oxyhydroxides, which can act as a sink for PTEs [9]. Furthermore, in estuarine systems, physicochemical conditions, such as pH, Eh, and salinity, and biogeochemical processes, such as adsorption, complexation, precipitation, and chelation, are affected by seasonal hydraulic changes like rainfall variations and water flow, which ultimately control the differentiation and mobility of PTEs [6,10–12].

Previous studies have demonstrated that sulfate reduction and concomitant metal sulfide precipitation can decrease PTE bioavailability in estuarine soils [1,3,4]. However, low sulfate concentrations in freshwater wetlands can impair metal sulfide formation [13]. Moreover, in redox-active environments (e.g., estuarine soils), the reductive dissolution of Fe oxyhydroxides may concomitantly release PTEs associated with these Fe minerals into the aqueous phase [12,14,15]. Therefore, Fe oxyhydroxides may act as a source of PTEs in the environment [10,14]. Because of the importance of these coupled interactions, more studies, including *in situ* research, are needed to address seasonal Fe geochemical changes and their impact on PTE dynamics in freshwater estuaries.

Here, we investigated the *in situ* seasonal changes in Fe dynamics and their control over PTE behavior in an estuary strongly impacted by Fe-rich mine tailings as a case study for the first time to understand how seasonal and temporal patterns affect a contaminated wetland system. Since 2015, the *Rio Doce* estuary has received Fe-rich mine tailings after the *Fundão* dam rupture in *Mariana* (*Minas Gerais*) [13,16,17]. In 2015, the *Fundão* dam rupture released more than 50 million cubic meters of iron mine tailings into the *Rio Doce* basin [18,19] The mine tailings traveled over 600 km until reaching the estuary 17 days after the dam rupture [18,19]. This disaster represents one of the largest failures of a tailings dam ever recorded, causing extensive ecological and cultural damage, as well as the death of 19 people [19]. Additionally, the total content of potentially toxic elements, such as Mn, Cr, Ni, Cu, and Pb, in the estuarine sediments increased by 2 to 5 times after the impact [16]. Given that, this estuary offers a unique framework for studying Fe reduction pathways under field conditions without the influence of sulfur because sulfate reduction is not favored owing to low seawater intrusion [13]. Moreover, seasonal soil biogeochemical changes have been poorly assessed in estuaries contaminated with mine tailings. Recent studies on estuarine bottom sediments have indicated that seasonal fluctuations may have a marked impact on metal contamination, resulting in health and ecological risks [17,18]. These impacts may be related to the high metal content derived from upstream river flow, which has continually transported tailings to the estuary since the dam collapsed in 2015 [19–21]. As the estuary receives most of the released tailings from the river basin, soil geochemical processes may play an essential role in retaining and releasing PTE associated with seasonal changes [11].

Therefore, alterations in soil geochemical characteristics are crucial for comprehending the retention and release of metals in estuarine soil systems and for predicting their environmental implications [10]. We hypothesized that greater water availability during the wet season would promote reduced soil conditions, favoring the dissolution of Fe oxides and hydroxides and the release of PTEs compared to the dry season. To test these hypotheses, we sampled soils from the Rio Doce Estuary in 2019 (dry season), 2020 (wet season), and 2021 (dry season) to evaluate the influence of seasonal changes on soil physicochemical parameters (pH and redox potential, Eh) and the bioavailability of soil Fe and PTEs.

2. Material and methods

2.1. Study area

The study area is located in the *Rio Doce* Estuary, *Espirito Santo* State, Brazil ([16]; Fig. 1A). The climate in the region is classified as Aw, according to the Köppen climate classification [22]. The annual average temperature is 22 °C and the fluvial regime follows the rainfall (Fig. 1B), showing two marked seasons: a wet season from November to March (rainfall 101–212 mm month^{-1} and historical streamflow average 965 m^3 s^{-1}) and a dry season from April to October (rainfall 53–97 mm month^{-1} and historical streamflow average 370 m^3 s^{-1}; [5,20]). In addition, the *Rio Doce* estuary typically has low salinities (0.05–0.65 ppt) throughout the year (see [17]).

2.2. Sampling and in-field measurements

Nine soil cores were collected during low tide in the same sampling sites for the field campaigns of August 2019 (dry season), January 2020 (wet season), and August 2021 (dry season) (Fig. 1). Soil sampling was performed using polyvinyl chloride tubes (PVC; 40 cm long with an internal diameter of 50 mm) previously washed with 10% HCl. After sampling, cores were hermetically stored at 4 °C in an upright position and taken to the laboratory, where the soil cores were sectioned in 5 cm intervals (0–5, 5–10, 10–15, and 15–20 cm), and stored at 4 °C.

Additional soil samples were collected using a semi-open-face auger at companion sites adjacent to core locations to obtain larger volumes of soil samples for analyses that did not require redox preservation (e.g., particle size distribution). At these locations, the pH and the redox potential (Eh) were measured in the field using a portable pH and ORP meter (Hanna®, model HI-991002, Hanna Instruments, Smithfield, RI, USA) previously calibrated with standard solutions (pH = 4, 7, and 10). The redox potentials were measured using a calomel reference and corrected to the standard hydrogen electrode reference state (+240 mV). The pH and Eh measurements were performed from 0 cm to 20 cm in 5 cm increments. After these measurements, the soil samples were placed in plastic bags, stored at 4 °C, and transported immediately to the laboratory for further processing.

2.3. Soil physicochemical and geochemical characterization

Soil organic matter content (SOM) was determined using the loss-on-ignition method following the elimination of inorganic carbon with 1 mol L^{-1} HCl, as described by [22]. Samples were initially weighed after drying at 105 °C, and then re-weighed after being heated at 450 °C

in a muffle furnace for 2 h, following the procedure outlined by [23]. For particle size determination, soil samples (collected using a face auger) were dried, homogenized, and sieved through a 2 mm mesh. The particles were separated and quantified using the sieve pipette method [24]. Briefly, samples were dispersed in 4% sodium hexametaphosphate for 16 h, and the sand was separated by sieving, and clay was separated from silt by pipetting based on Stokes' law.

The geochemical fractionation of Fe and PTEs (Mn, Cr, Cu, Ni and Pb) was performed using fresh soil samples (collected in PVC tubes). Two grams of soil were taken from the center of each core to avoid contact with atmospheric air. To prepare the solution, type 1 ultrapure water was bubbled with N_2 for one hour, and the extractant solutions were prepared using high-purity chemicals (at least 99% purity). Six operationally different fractions [2,24] were sequentially obtained.

1 Exchangeable and soluble Fe and PTEs (EX): The sample (1.0 g) was shaken for 30 min in 30 ml of 1 mol L^{-1} $MgCl_2$ solution (pH 7.0).

2CA-Fe and PTEs associated with carbonates were shaken for 5 h in 30 ml of 1 mol L^{-1} sodium acetate solution (pH 5.0).

3FR – Fe and PTEs associated with ferrihydrite: shaken for 6 h at 30 °C in 30 ml of 0.04 mol L^{-1} hydroxylamine + 25% acetic acid (vol/vol) solution.

4LP – Fe and PTEs associated with lepidocrocite: shaken for 6 h at 96 °C in 30 ml of 0.04 mol L^{-1} hydroxylamine + 25% acetic acid (vol/vol) solution.

5CO - Fe and PTEs associated with crystalline Fe oxyhydroxides (e.g., goethite and hematite): shaken for 30 min at 75 °C in 20 ml of 0.25 mol L^{-1} sodium citrate + 0.11 mol L^{-1} sodium bicarbonate with 3 g of sodium dithionite.

6PY - Pyritic Fe (PY): after eliminating the Fe and PTEs associated with silicates using 10 mol L^{-1} HF and the organic phase using concentrated H_2SO_4, the pyritic phase was extracted by shaking the residue for 2 h at room temperature with 10 ml of conc. HNO_3.

The easily available (EA) fraction was considered the sum of fractions 1 and 2 (i.e., EX and CA contents) [25,26]. The pool of Fe associated with short-range ordered Fe oxides (SRO) were considered the sum of the fractions 3 and 4 (i.e., FR and LP contents). The pseudo-total concentrations of Fe and other PTEs (Mn, Cr, Cu, Ni and Pb) were calculated as the sum of all fractions.

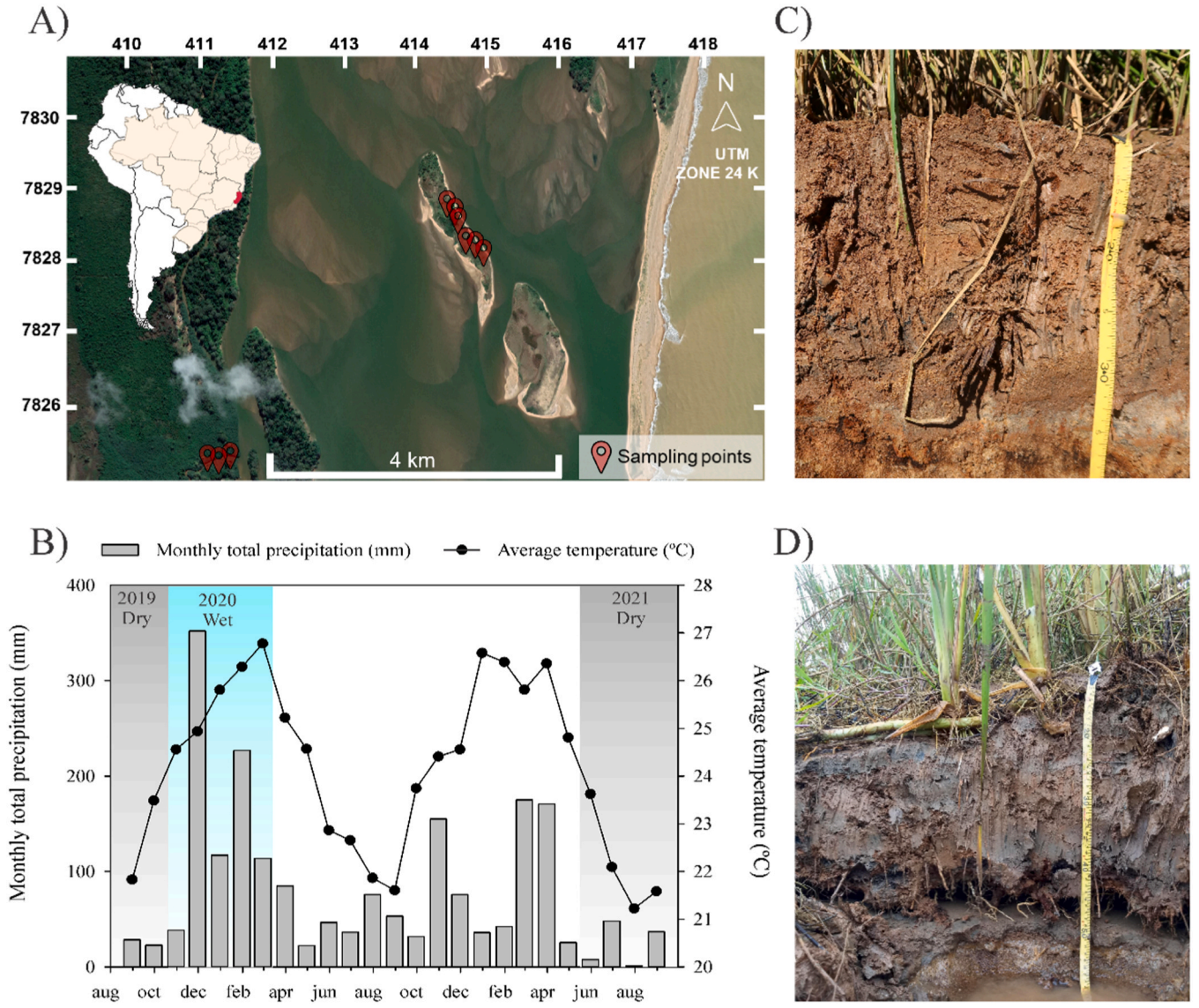

Fig. 1. A. Sampling locations at the *Rio Doce* estuary (A; n = 9); B. Annual variability in precipitation and temperature in the estuarine region during the sampling period (April 2019 to October 2021). C. Soil profile in the 2019 dry season. D. Soil profile of the 2020 wet season. Climate data were obtained from the Brazilian National Institute of Meteorology (Inmet) database. Data were collected from an automatic station (A614) in Linhares, Espirito Santo, Brazil.

2.4. Fe and PTEs determination in analytical extracts

The Fe and other PTE concentrations in the extracts were determined in triplicate by using inductively coupled plasma-optical emission spectrometry (ICP-OES, 1Cap6300 Duo model, Thermo Fisher Scientific®, Waltham, MA, USA) according to the 6010 C protocol from USEPA [27]. Calibration solutions were prepared by diluting certified standard solutions (Sigma–Aldrich, St. Louis, MO, USA). For quality assurance, certified reference solutions were used as analytical check standards, with the measured values varying between 90% and 110% of the known values.

2.5. Statistical analysis

Because the data did not show a normal distribution, the soil parameters (pH, Eh, particle size, and Fe and PTEs pseudo-total contents and fractions) were compared between seasons (dry 2019, wet 2020, and dry 2021) using the Kruskal-Wallis non-parametric test, and averages (n = 36; nine sites per season × four depths of soil collection per site) were compared using the Dunn test (Table S1). Principal component analysis (PCA) was applied to the data obtained in two contrasting seasons (wet season, January 2020, and dry season, August 2019 and 2021) to explain the data variability through soil variable modeling (pH, Eh, particle size distribution, and geochemical fractionation of Fe and other PTEs) using a linear combination of factors and error terms (Table S3). The variables kept were chosen to maximize the explained variability in the lowest number of components possible. To guarantee the reliability of the analysis, a parallel analysis was done to test how many PCs are significant. The bootstrap resampling (number of interactions equal to 1000) was applied to guarantee data normality during parallel analysis. In addition, mixed-effects linear models were developed to predict the parameters that could exert control over PTEs bioavailability through stepwise backward elimination. The parameters were divided into three categories: i) climatic data (monthly average temperature and total precipitation), ii) soil physical and chemical attributes (clay content, pH, potential redox potential, and organic matter content), and iii) soil geochemical attributes (pools of geochemical fractionation: EX, CA, FR, LP, CO, and PY). The significant variables in each equation were selected to express the highest conditional R^2 and Akaike's information criterion (AIC), minimizing data loss (Table S3). All statistical analyses were performed using R software ([28]).

3. Results

3.1. Seasonal effects on soil physicochemical conditions and particle-size distribution

The soil organic matter content did not differ between the seasons (Table S1) and were, on average, 15.2% (Fig. S2). Soil particle size changed significantly over time (Fig. 2; Table S1), particularly in the upper layer (0–5 cm). Fine particles (clay content) increased from 299 g kg^{-1} during the dry season (2019) to 441 g kg^{-1} during the wet season (2020; Fig. 2). The only layer with a significant increase in clay contents was the upper soil layer (0–5 cm) (Table S1). In the following dry season (2021) fine particles content remained at 441 g kg^{-1} (Fig. 2).

Physicochemical parameters (pH and Eh) also showed clear seasonal fluctuations (Fig. 3A; Table S1). In the dry seasons of 2019 and 2021, mean pH values recorded were 5.2 ± 0.2 (Fig. 3A). In contrast, during the wet season of 2020, pH was 6.2 ± 0.4 (Fig. 3A). In contrast, the Eh values were higher during the dry seasons (+290 ± 92 mV) when compared to the wet season (−40 ± 170 mV; Fig. 3B; Table S1).

3.2. Seasonal effects on pseudo total contents of Fe and PTEs

The pseudo-total Fe content in the *Rio Doce* estuarine soil also changed seasonally (Fig. 4). The pseudo-total Fe contents was 2.7-fold

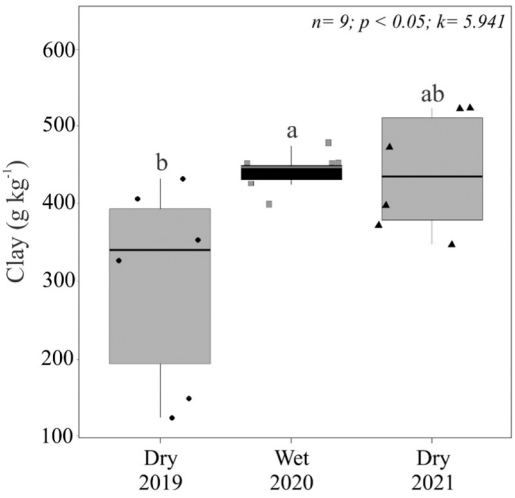

Fig. 2. Soil clay contents in samples from the soil surface (0–5 cm) during the three studied seasons at Rio Doce estuary. Medians followed by the same letter did not differ from the non-parametric Kruskal-Wallis test (p > 0.05).

higher in the 2020 wet season (50.5 g kg^{-1}; Fig. 4A) than in the dry seasons of both 2019 and 2021 (18.7 g kg^{-1}; Fig. 4A). The pseudo-total Mn content in soils was 1.6-fold higher in the wet season of 2020 (420 mg kg^{-1}; Fig. 4B) than in the dry season (264 mg kg^{-1}; Fig. 4B).

Similar to the concentrations of Fe and Mn, Cr and Ni showed higher pseudo-total concentrations during the wet season (Figs. 4C and 4E). Cr contents in the soils during the 2020 wet season were 1.9-fold higher (49.9 mg kg^{-1}, Fig. 4C) than in the dry seasons (25.9 mg kg^{-1}, Fig. 4C). Similarly, the Ni content in the soils during the 2020 wet season was 1.4-fold higher (5.7 mg kg^{-1}, Fig. 4E) than that in the dry season (4.0 mg kg^{-1}, Fig. 4E). Soil Cu pseudo-total content was higher in the 2020 wet season (12.7 mg kg^{-1}; Fig. 4D), with lower contents in the 2019's dry season. Similarly to Cu total contents in soils, for Pb there was a 99% increase in its total pseudo content between the dry season of 2019 (11.1 mg kg^{-1}; Fig. 4F) and the following wet season (22.1 mg kg^{-1}; Fig. 4F). Between the 2020 wet season and the next dry season, the Pb pseudo-total content did not change (20.2 mg kg^{-1}; Fig. 4F).

3.3. Seasonal effects on the geochemical partitioning of Fe and PTEs

Fe concentrations in the different soil fractions are shown in Fig. 5. The Fe oxide (short-range ordered SRO and crystalline oxide-CO) fractions were predominant, comprising more than 99% of the extractable Fe. In addition, all the Fe fractions (easily available and associated with Fe oxides) exhibited clear seasonal trends (Fig. 5). Greater EA-Fe contents were observed during the dry seasons (103.2 mg kg^{-1}; Fig. 5A) than in the wet season (17.2 mg kg^{-1}; Fig. 5A). In contrast, the SRO-Fe content was higher in the wet season (14,000 mg kg^{-1}; Fig. 5B) than in the dry season (6368 mg kg^{-1}; Fig. 5B). This pattern was also observed for CO, with greater Fe content in the wet season of 2020 (36,444 mg kg^{-1}; Fig. 5C) than in the dry season (12,176 mg kg^{-1}; Fig. 5C).

In contrast to Fe, the geochemical fractions of Mn showed different seasonal trends (Fig. 6). The readily available Mn (Mn-EA) contents in soils decreased over time, with the dry season of 2019 (59.8 mg kg^{-1}; Fig. 6A) exceeding the 2020 wet (37.7 mg kg^{-1}; Fig. 6A) and the 2021 dry (35.2 mg kg^{-1}; Fig. 6A) seasons. In contrast, the soil contents of Mn associated with short-range ordered oxides (Mn-SRO), as with the total Mn contents (Fig. 5B), did not change significantly and averaged 223.7 mg kg^{-1} (Fig. 6B). The soil content of Mn associated with crystalline oxides (Mn-CO) was greater in the 2020 wet season (100.3 mg kg^{-1}; Fig. 6C) than in the dry seasons (22.5 mg kg^{-1};

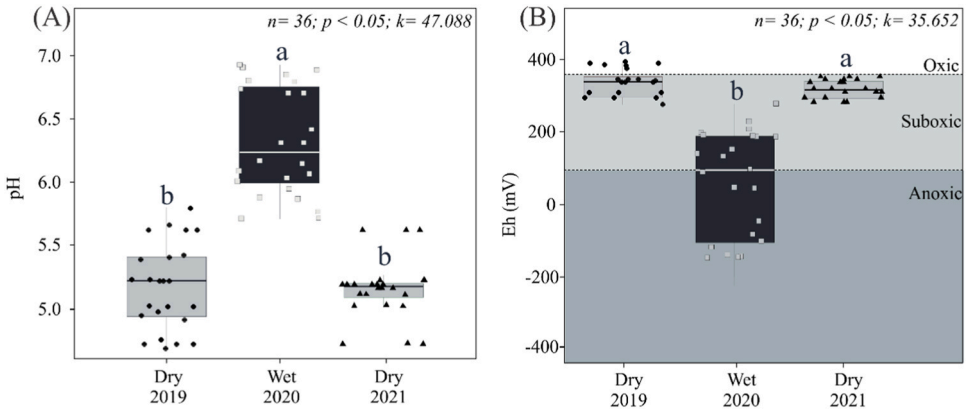

Fig. 3. Soil pH (A) and redox potential (Eh; B) during the different seasons at *Rio Doce* estuary. Soil depths totaled 36 replications (9 sites × 4 depths). Dotted lines and shadow areas delimited geochemical environments, according to Otero et al. (2009). Medians followed by the same letter did not differ from the non-parametric Kruskal-Wallis test ($p > 0.05$).

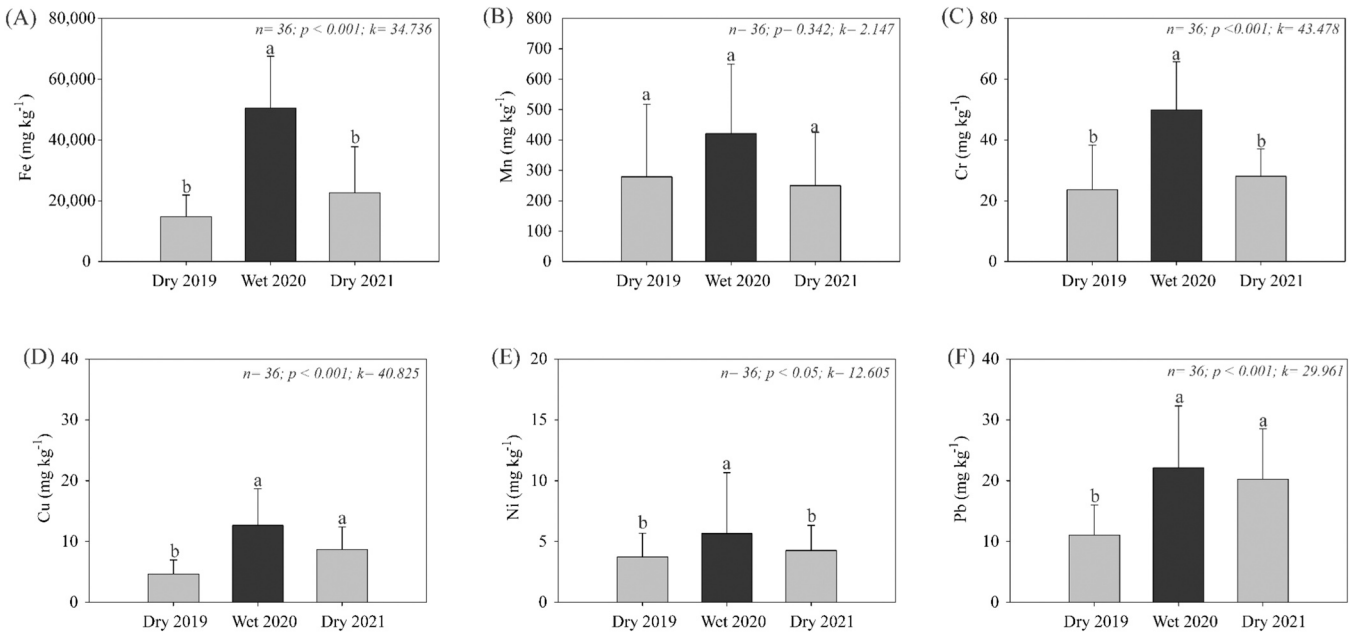

Fig. 4. Pseudo-total concentrations of Fe (A), Mn (B), Cr (C), Cu (D), Ni (E), and Pb (F) in the soils of *Rio Doce* estuary during the different seasons of 2019 to 2021. Medians followed by the same letter did not differ from the non-parametric Kruskal-Wallis test ($p > 0.05$).

Fig. 6C).

The PTEs associated with short-range ordered oxides (SRO) were significantly affected by seasonality, showing higher concentrations in the wet season for all the PTEs studied (Figs. 7B, 7E, 7H, and 7 K). This pattern mirrors the trends observed for the Fe and Mn SRO fractions (cf. Figs. 5 and 6). However, the crystalline oxide fraction (CO) did not show the same pattern for all the PTEs. A higher Cr-CO content in the soil was recorded in the wet season than in the dry season (Fig. 7C). The Cu-CO content increased 8.5-fold between 2019 and 2021 (Fig. 7F). In contrast, the Ni-CO contents decreased 3-fold during the same period (Fig. 7I). Pb-CO did not change over time, with values averaging 2.1 mg kg^{-1} (Fig. 7A). The soil content of readily available fractions (i.e., EX and CA) increased over time for all PTEs, except Cr (Figs. 7A, 7D, 7G, and 7 J). Cr-EA contents decreased 4.1-fold between 2019 (1.7 mg kg^{-1}; Fig. 7A) and 2021 (0.4 mg kg^{-1}; Fig. 7A), whereas Cu, Ni, and Pb increased 2.9, 6.6, and 1.9-fold over time, respectively (Figs., 7D, 7 G, and 7 J).

3.4. Modeling of seasonal effects on the readily available contents of PTEs

Linear regression using stepwise backward elimination resulted in four equations for predicting the readily available Mn, Cr, Ni, and Pb content (i.e., EA-Mn, EA-Cr, EA-Ni, and EA-Pb) in the studied estuarine soils (Table 1). Modeling showed that climatic data (i.e., monthly average temperature in Celsius degree and total precipitation in mm) contributed 48% of the total weight (Fig. S1; Table S2), followed by physical and chemical data (pH, Eh, and soil organic matter, contributing 29%; Fig. S1; Table S2) and geochemical fractions (23%; Fig. S1; Table S2). Total precipitation was the most important climatic factor for all EA-PTEs studied, whereas soil organic matter content (Fig. S2) and pH were the most critical physicochemical factors (Table 1). Regarding geochemical factors, more available fractions (Fe-EX and Fe-CA) exerted significant control over the contents of easily available PTEs and short-range ordered oxides (FR and LP), which also contributed positively to higher EA-PTEs contents (Table 1).

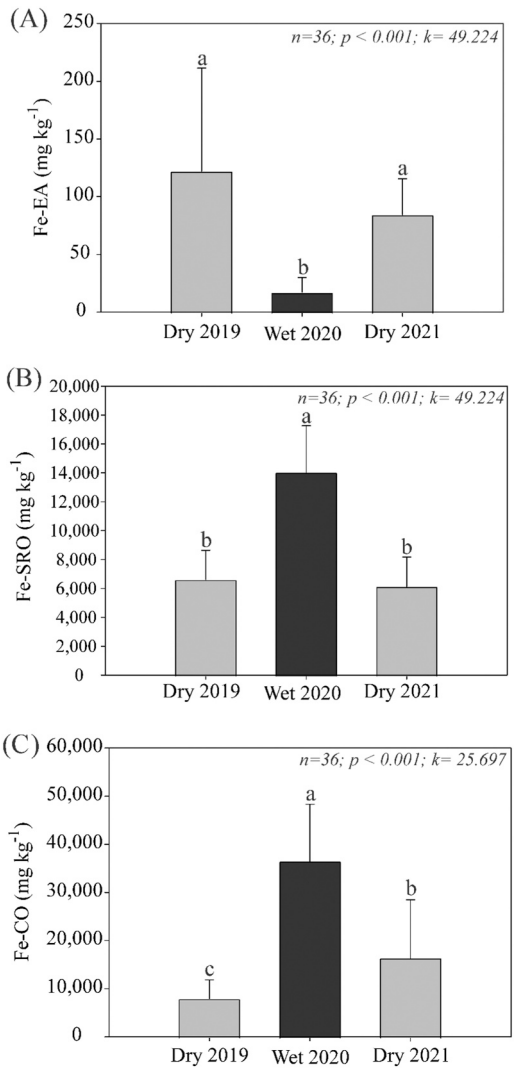

Fig. 5. Seasonal changes in the different geochemical fractions of Fe in soils from the *Rio Doce* estuary during the different seasons from 2019 to 2021. EA- readily available (A); SRO- short-range ordered oxides (B) and CO- crystalline oxides (C). Medians followed by the same letter did not differ from the non-parametric Kruskal-Wallis test ($p > 0.05$).

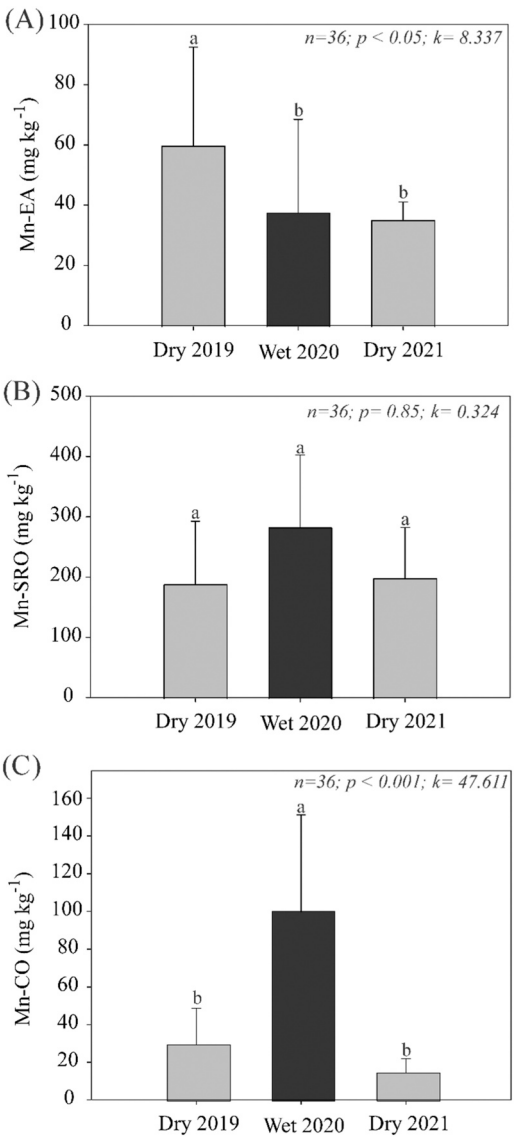

Fig. 6. Seasonal changes in the different geochemical fractions of Mn in soils from *Rio Doce* estuary in the different seasons from 2019 to 2021. EA- readily available (A); SRO- short-range ordered oxides (B) and CO- crystalline oxides (C). Medians followed by the same letter did not differ from the non-parametric Kruskal-Wallis test ($p > 0.05$).

3.5. Principal component analysis (PCA)

Data variability was constrained by two principal components that explained 66.1% of the variance (Table S4). Principal component 1 (PC1) accounted for 44.8% of the variance and showed a contrast between the total precipitation, pH, clay content, Cr-SRO, Cu-SRO, Ni-SRO, Pb-SRO, Fe-OX, Eh, sand content, and Fe-SRO (Fig. 8). Principal component 2 (PC2) explained 21.3% of the total variance and had maximum positive loadings for Eh and sand content and negative loadings for clay content and pH (Fig. 8).

4. Discussion

4.1. Seasonal control over the physical and chemical environment

Our results showed a clear seasonal effect on soil composition and physicochemical properties (i.e., soil particle size, pH, and Eh; Figs. 2 and 3; Table S1). The *Rio Doce* Basin has greater fluvial discharge, turbidity, and total suspended solid content during the wet season than during the dry season [19,21], favoring soil estuarine accretion. Queiroz et al. [15] showed a thickening of soils formed at the *Rio Doce* Estuary toward the surface by adding mineral particles, mainly fine particles, especially crystalline Fe oxides Fe-OX, due to mine tailing transportation from the river basin to the estuary.

By comparing the particle size distribution along the *Rio Doce* Basin before and after the *Fundão* Dam rupture, Duarte et al. [29] found that Fe mine tailings, predominantly silt–clay, were incorporated into the original sandy river sediments, altering the particle size composition of estuarine soils. Mixed silt-clayey can be carried downstream, particularly during seasonal flooding in the wet season (Fig. 2). Thus, an increase in the fine particle content, especially on the soil surface, is associated with the seasonal deposition of Fe mine tailings after dam rupture [13,15–17,29]. Mixed silt-clayey material deposition can affect soil properties, ecosystem structure, and function [30]. For instance, higher fine particle contents can lead to higher soil cation exchange capacity (CEC) owing to the high surface area of silt-clayey material [31], which affects the retention capacity of PTEs in soils. In addition, fine particle deposition favored plant colonization on islands that were not vegetated before the disaster, increasing the soil's organic carbon

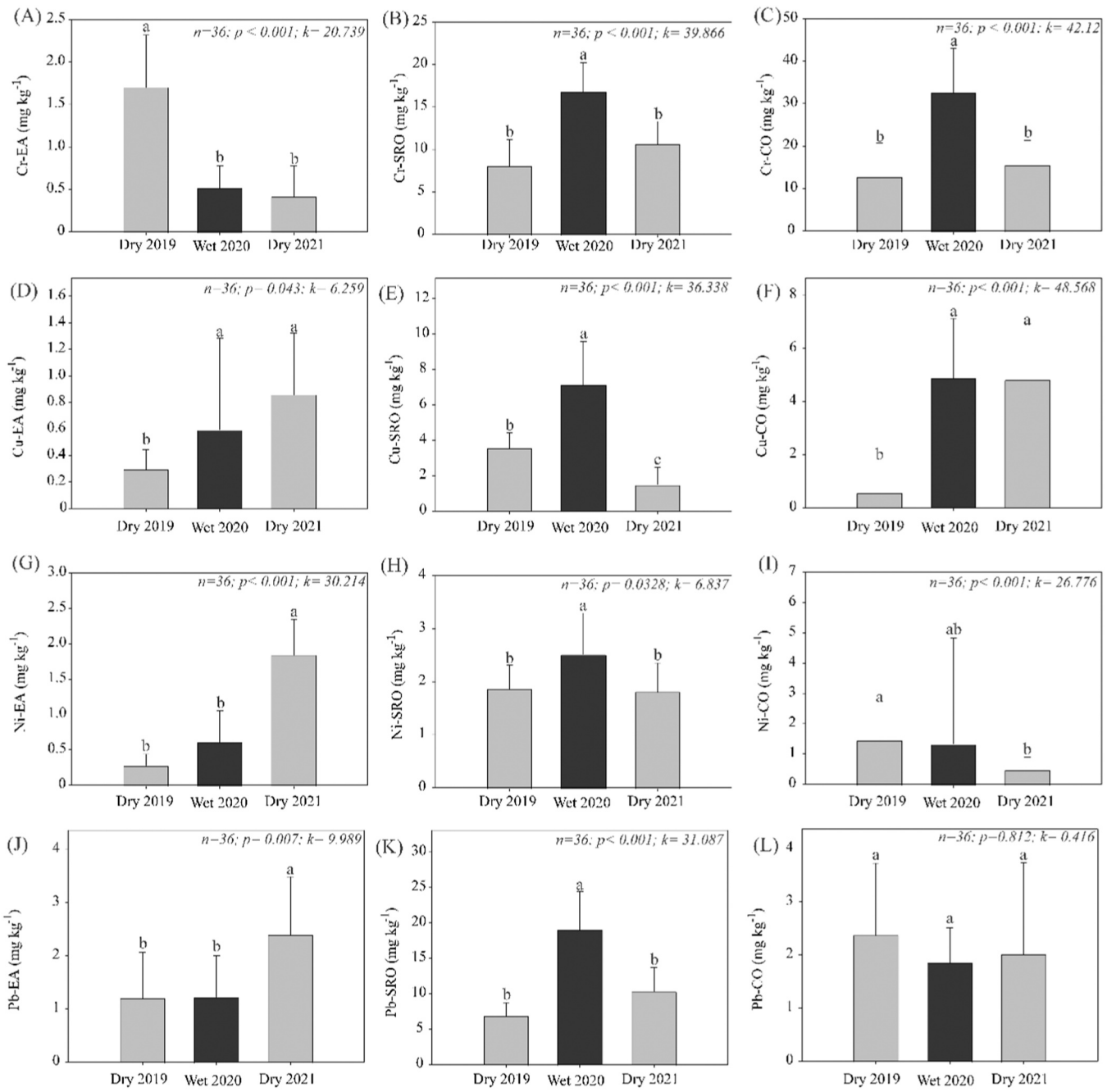

Fig. 7. Seasonal changes in the different geochemical fractions of PTEs in soils from *Rio Doce* estuary in the different seasons from 2019 to 2021. EA- readily available (A, D, G, and J); SRO- short-range ordered oxides (B, E, H, and K) and CO- crystalline oxides (C, F, I and L). Medians followed by the same letter did not differ from the non-parametric Kruskal-Wallis test ($p > 0.05$).

contents (see [15]).

Seasonality also influenced pH and Eh (Fig. 3). Lower redox potentials were observed in soils during the wet season (Fig. 3B). Higher river discharge can explain the maintenance of suboxic and anoxic soil environments because it increases soil waterlogging and reduces aeration [6,32]. The oxygen diffusion rate in water-filled pores drastically decreases [33], causing microorganisms to use anaerobic pathways for organic matter oxidation. Alternative electron acceptors will be used (e.g., oxides and hydroxides of Fe and Mn), and reducing conditions will be established [34,35]. Suboxic/anoxic conditions also explain the more alkaline pH during the wet season (Fig. 3A) because the reduction reactions consume protons, leading to a circumneutral pH (see Eqs. 1 and 2; [4]). This close relationship between pH and Eh was highlighted by the higher loads and opposite directions between the pH and Eh vectors for Factor 2 (Fig. 8, Table S3).

$$Fe_3O_4 + 8\,H^+ + 2\,e^- \rightarrow 3\,Fe^{2+} + 4\,H_2O \quad (1)$$

$$MnO_2 + 4\,H^+ + 2\,e^- \rightarrow Mn^{2+} + 2\,H_2O \quad (2)$$

We found that the *Rio Doce* estuarine soils maintained suboxic conditions continuously during the dry season (i.e., $+350 > Eh > +100$ mV; Fig. 3B). This could be a result of the mixed silt–clay material overlying the sand material (Fig. S3). Vepraskas et al. [36] showed that the water content could remain high, and Fe-reducing conditions could occur even under unsaturated conditions if silty clay loam material overlies coarse sand because fine-textured materials can hold water owing to their

Table 1
Summary of the mixed-effect linear model for PTEs bioavailability obtained via stepwise backward elimination* .

Dependent Variable	Equation	R^2
EA-Mn	0.029 *PREC − 1.53 *SOM + 0.16 *Fe-CA + 0.01 *Fe-FR + 0.13 *Mn-FR - 0.14 *Mn-LP + 35.9	0.623
EA-Cr	1.52 *PREC - 0.005*TEMP - 0.52 *pH + 0.013*Fe-EX + 0.225 *Cr-FR - 0.32	0.624
EA-Ni	1.92 *PREC - 0.006 *TEMP + 0.54 *Ni-FR + 44.3	0.408
EA-Pb	0.013 *PREC - 0.0001 *Fe-CO + 0.27 *Pb-FR + 0.14 *Pb-LP + 1.306	0.367

*AIC, F-statistic, and RSE are presented in Supplementary Information (Table S3). EA: easily available fractions (sum of exchangeable and carbonate-associated contents in mg kg^{-1}); PREC: total precipitation in mm; TEMP: average temperature in Celsius degree; SOM: soil organic matter content in %; CA: Fe and other metals associated with carbonates in mg kg^{-1}; FR: Fe and other metals associated with ferrihydrite in mg kg^{-1}; LP: Fe and other metals associated with lepidocrocite in mg kg^{-1}; CO: Fe and other metals associated with well-ordered oxides (e.g., hematite and goethite) in mg kg^{-1}.

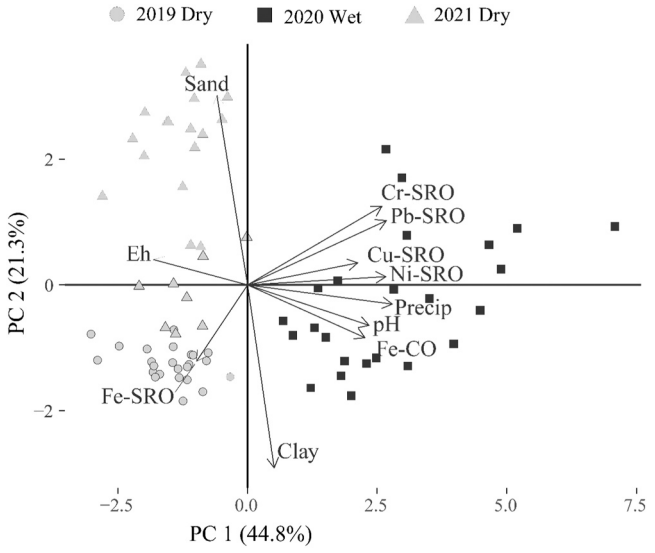

Fig. 8. Principal component analysis of climatic data (monthly total precipitation), soil physicochemical parameters (pH, redox potential - Eh), particle size distribution, and geochemical fractions of Fe and other PTEs in estuarine soils at three seasons (wet - January 2020; and dry seasons - August 2019 and August 2021). CO: crystalline Fe oxides; SRO: short-range ordered Fe oxides. Variables were selected to maximize the data variability explained.

matrix potential, preventing downward movement until full saturation [36]. Daily soil flooding due to tidal effects, especially in deeper layers [15] and continuous carbon addition to the soil by plants [15] also contribute to suboxic conditions.

The lower pH observed during the dry season results from the oxidation of reduced species, the release of protons (e.g., Fe^{2+} form; Eq. 3), and the formation of SRO Fe oxides [4,37,38]. The role of acidic root exudates in proton production must also be considered [39,40]. Under slightly acidic conditions (pH ~5), further solubilization of SRO Fe oxides can occur, releasing the adsorbed PTEs. Slightly acidic conditions maintain the dissolved metallic cationic species (e.g., Ni, Cr, Cu, and Pb), contributing to their removal.

$$Fe^{2+} + ¼\ O_2 + 3/2\ H_2O \rightarrow FeOOH + 2\ H^+ \quad (3)$$

4.2. Seasonal control over Fe geochemistry in estuarine soils impacted by mine tailings

The seasonal deposition of Fe-enriched fine particles affected the pseudo-total Fe content and Fe geochemical partitioning (Figs. 4 and 5). The Fe pseudo-total content increased 3.4-fold from the 2019 dry season to the 2020 wet season (Fig. 4A), as Fe-rich tailings, mainly composed of Fe oxides, were preferentially deposited during the wet season (Figs. 5B and 5C). Furthermore, in the first few days after the arrival of mine tailings in the estuary, the Fe content increased in the soil surface (0–3 cm) compared to deeper soil layers (e.g., 15–30 cm), which were composed mainly of sand [13,16]. Thus, the predominance of Fe-CO forms in the wet season (average: 72%; Fig. 5C) is consistent with the seasonal deposition of mixed silt-clayey material. Indeed, Queiroz et al. [15] reported that newly deposited tailings in estuarine soils were mainly composed of Fe-CO two years after the disaster. These Fe minerals are less prone to reductive dissolution than SRO Fe oxides [4,41]. In addition, the circumneutral pH during the wet season (Fig. 3A) can provide a geochemically stable environment for recently deposited Fe oxides (Gotoh and Patrick, 1974). However, seasonal variability in the estuarine soil physicochemical environment favored Fe-reducing conditions (i.e., suboxic and acidic conditions in the dry seasons; Fig. 3), which resulted in significant losses of Fe between the 2020 wet season and 2021 dry season (−55%, Fig. 4A).

From the wet to the dry season, the Fe-CO pools likely dissolved to Fe^{2+}, which could be incorporated into the EA-Fe pools (Fig. 5A). However, dissolved Fe can also precipitate as SRO fractions (e.g., on hot spots of oxygen, such as surrounding roots). During the 2020 (wet season), SRO represented 28% of the pseudo-total Fe content, whereas in the dry seasons (2019 and 2021), it represented 36% of the total Fe content and became the main fraction (Fig. 5B).

Redox fluctuations during the dry season may enhance the SRO precipitation [42,43]. Higher temperatures during the dry season (Fig. 1B) may increase the evapotranspiration of estuarine plants [44,45], which can reduce the water content in soils [46], increase Eh [47] and promote a favorable environment for SRO Fe oxide precipitation.

4.3. Seasonality of Fe geochemistry and its control over the fate of PTEs

The seasonal effects of Fe geochemistry also affect the dynamics of other PTEs [7,8]. Our findings indicate a clear seasonal effect on the total content (Fig. 5), with a significant increase from the dry season to the wet season and a decrease from the wet season to the next dry season (Fig. 5). The arrival of Fe-rich crystalline fine materials (Figs. 3, 4, and 5A) during the wet season could immobilize PTEs. However, the loss of Fe (~ 47 g kg^{-1} of released Fe; Fig. 5) from the wet season to the following dry season indicated the potential dissolutive reduction of Fe oxides. Thus, in the dry season, Fe-SRO and Fe-CO can temporarily control PTE bioavailability because, in the following dry season, most of this fraction undergoes reductive dissolution (Fig. 5).

Continuous PTE release poses hazards to the biota over time, as the EA content of Cu, Ni, and Pb increased, on average, by 281% in two years (Fig. 6). This increase probably resulted from the decrease in Fe crystallinity over time, leading to a high susceptibility to the dissolution of the SRO Fe forms [10,15]. Therefore, our findings revealed that seasonality exerts an essential control on estuarine soils contaminated by mine tailings, altering their capacity to immobilize PTEs (Table 1, Fig. S1). This was further corroborated by the higher contribution of climatic factors, mainly precipitation, to PTEs bioavailability modeling (48% of the models were explained by precipitation and temperature data).

Climatic factors affected the physicochemical environment (Figs. 2 and 3), and pH was a significant driver of PTE availability (Table 1). Physicochemical factors like pH affect the maintenance of Fe oxide in the wet season, whereas a lower pH favors Fe losses in the dry season. The modeling showed that Fe and other PTEs associated with SRO forms

had higher loads on geochemical factors, highlighting the crucial role of these fractions in PTE bioavailability (Table 1). During the dry season, an acidic and suboxic soil environment (Fig. 3B) enhanced Fe oxide dissolution (SRO and CO forms), promoting its decrease in the soil (Fig. 6) and its release into the water, which could potentially decrease the water quality of *Rio Doce* in the estuary.

Based on our findings, we propose the following conceptual model (Fig. 9): during the wet season, fine particles, mainly composed of crystalline Fe oxyhydroxides, can be deposited in estuarine soils. From the wet to the dry season, Fe oxyhydroxides probably dissolve due to acidic and suboxic conditions, and then release both Fe and the associated PTEs (e.g., Mn, Cr, Cu, Ni, and Pb), decreasing their pseudo-total contents, and increasing their bioavailability. In the following dry season, short-range ordered Fe and Mn oxyhydroxide (SRO) precipitation can occur because of short oxic periods, especially near the root channels, favoring PTE adsorption in these fractions. However, these SROs are more prone to redissolution, which can increase the potential mobility of PTEs in estuarine soils. This scenario could explain the high losses of Fe, Mn, Cr, Cu, Ni, and Pb from soils during the wet and dry seasons (Fig. 5), posing severe risks to estuarine environmental health.

5. Concluding remarks and environmental implications

The estuarine soil geochemical environment was affected by seasonal changes (precipitation), which also affected Fe oxyhydroxide dynamics and its capacity to retain PTEs such as Mn, Cr, Cu, Ni, and Pb. From the wet to dry seasons, Fe oxide dissolution promoted a decrease in the pseudo-total Fe content, representing a loss of 79% over the two years. Furthermore, we observed a 281% increase in easily available forms of PTEs in two years, elevating environmental risks, especially during the dry season. Fishing is an important economic activity in the region and has been banned since the arrival of tailings in the estuaries in 2015. This study can help regulate artisanal and professional fishing by defining times of lower risk for carrying out these activities.

Although several studies have shown that estuarine soils can act as sinks for PTEs [48,49], our data indicated that this depends on the seasons (Table 1). Our data showed a loss of Fe and other PTEs from the wet to the dry season (Fig. 3) of up to 65.7 ton ha^{-1} of Fe, coupled with significant losses of Mn (216 kg ha^{-1}), Cr (30.6 kg ha^{-1}), Cu (5.6 kg ha^{-1}), Pb (2.6 kg ha^{-1}) and Ni (2.0 kg ha^{-1}). These losses can potentially affect estuarine environments and serve as sources of iron and PTEs in the ocean. Our data suggest that the intensity of this contribution is markedly affected by season and could affect the ecosystem services provided by these environments (e.g., carbon and PTEs sequestration). Finally, the present work underscores the significance of conducting seasonal studies to understand real-time geochemical dynamics in estuarine soils better. This approach contrasts studies employing a "snapshot" methodology, which relies on single campaign-based sampling.

CRediT authorship contribution statement

Amanda Duim Ferreira: Writing – original draft, Methodology, Investigation, Formal analysis, Data curation, Conceptualization. **Owen W. Duckworth:** Writing – review & editing, Validation, Supervision, Project administration. **Hermano Melo Queiroz:** Writing – review & editing, Methodology, Formal analysis. **Gabriel Nuto Nóbrega:** Writing – review & editing. **Diego Barcellos:** Writing – review & editing, Validation, Data curation. **Ângelo Fraga Bernardino:** Writing – review & editing, Project administration, Investigation, Funding acquisition. **Xosé L Otero:** Writing – review & editing, Project administration, Funding acquisition. **Tiago Osório Ferreira:** Writing – review & editing, Supervision, Project administration, Methodology, Funding acquisition, Conceptualization.

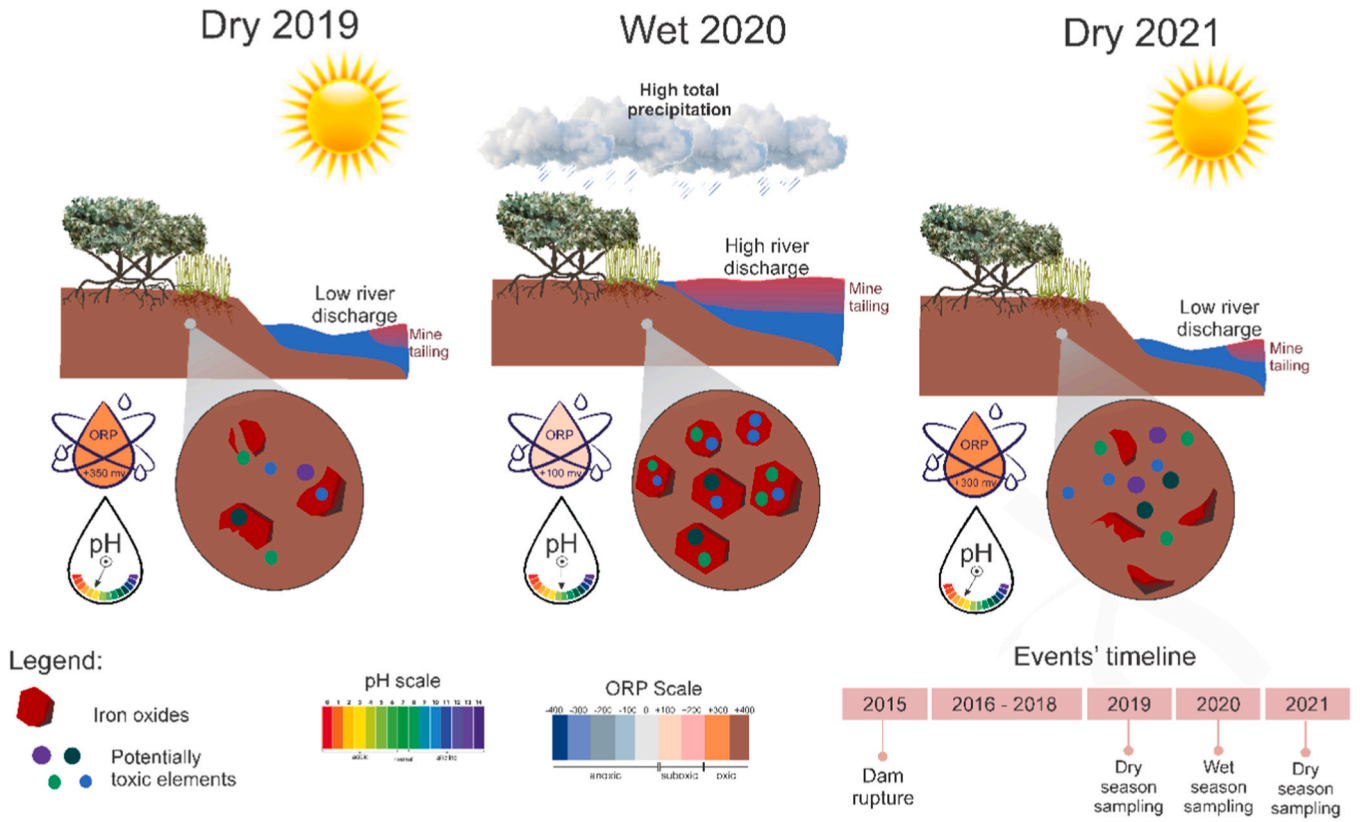

Fig. 9. Conceptual model of seasonal geochemical changes in the estuarine soils impacted by iron-rich mine tailings.

Declaration of Competing Interest

The authors declare that they have no known competing financial interests or personal relationships that could have appeared to influence the work reported in this paper.

Data availability

Data will be made available on request.

Acknowledgments

The authors appreciate the valuable comments on an earlier draft of this manuscript by Dr. Michael J. Vepraskas. This work received financial support from Fundação de Amparo à Pesquisa do Estado de São Paulo (FAPESP, grant numbers ADF: 19/14800–5; DB: 19/02855–0; HMQ: 21/00221–3; TOF: 19/19987–6; 22/12966-6); Fundação de Amparo do Espírito Santo (FAPES/CNPq/CAPES Rio Doce 77683544/2017); Coordenação de Aperfeiçoamento de Pessoal de Nível Superior CAPES—Finance Code 001 and Conselho Nacional de Desenvolvimento Científico e Tecnológico (grant numbers, AFB: 301161/2017–8, TOF: 305013/2022–0, GNN: 409593/2018–4). XLO was supported by the Department of Education and University Planning of Galicia (GRC GI 1574) and the CRETUS Strategic Group (AGRUP2015/02). The O.W.D. was supported by the USDA National Institute of Food and Agriculture (Hatch Project, NC02713). The FUNCAP Chief Scientist Fellowship supported the GNN.

Appendix A. Supporting information

Supplementary data associated with this article can be found in the online version at doi:10.1016/j.jhazmat.2024.134592.

References

[1] Ponting, J., Kelly, T.J., Verhoef, A., Watts, M.J., Sizmur, T., 2021. The impact of increased flooding occurrence on the mobility of potentially toxic elements in floodplain soil – a review. Sci Total Environ 754, 142040. https://doi.org/10.1016/J.SCITOTENV.2020.142040.

[2] Ferreira, T.O., Otero, X.L., Vidal-Torrado, P., Macías, F., 2007. Effects of bioturbation by root and crab activity on iron and sulfur biogeochemistry in mangrove substrate. Geoderma 142, 36–46. https://doi.org/10.1016/J.GEODERMA.2007.07.010.

[3] Ponting, J., Verhoef, A., Watts, M.J., Sizmur, T., 2022. Field observations to establish the impact of fluvial flooding on potentially toxic element (PTE) mobility in floodplain soils. Sci Total Environ 811, 151378. https://doi.org/10.1016/J.SCITOTENV.2021.151378.

[4] Du Laing, G., Rinklebe, J., Vandecasteele, B., Meers, E., Tack, F.M.G., 2009. Trace metal behaviour in estuarine and riverine floodplain soils and sediments: a review. Sci Total Environ 407, 3972–3985. https://doi.org/10.1016/J.SCITOTENV.2008.07.025.

[5] Bernardino, A.F., Netto, S.A., Pagliosa, P.R., Barros, F., Christofoletti, R.A., Rosa Filho, J.S., Colling, A., Lana, P.C., 2015. Predicting ecological changes on benthic estuarine assemblages through decadal climate trends along Brazilian Marine Ecoregions. Estuar Coast Shelf Sci 166, 74–82. https://doi.org/10.1016/J.ECSS.2015.05.021.

[6] Steinman, A.D., Ogdahl, M.E., Weinert, M., Thompson, K., Cooper, M.J., Uzarski, D.G., 2012. Water level fluctuation and sediment–water nutrient exchange in Great Lakes coastal wetlands. J Gt Lakes Res 38, 766–775. https://doi.org/10.1016/J.JGLR.2012.09.020.

[7] Otero, X.L., Macías, F., 2002. Spatial and seasonal variation in heavy metals in interstitial water of salt marsh soils. Environ Pollut 120, 183–190. https://doi.org/10.1016/S0269-7491(02)00159-8.

[8] Otero, X.L., Macias, F., 2003. Spatial variation in pyritization of trace metals in salt-marsh soils. Biogeochemistry 62, 59–86. https://doi.org/10.1023/A:1021115211165/METRICS.

[9] Komárek, M., Vaněk, A., Ettler, V., 2013. Chemical stabilization of metals and arsenic in contaminated soils using oxides – a review. Environ Pollut 172, 9–22. https://doi.org/10.1016/J.ENVPOL.2012.07.045.

[10] Barcellos, D., Queiroz, H.M., Ferreira, A.D., Bernardino, A.F., Nóbrega, G.N., Otero, X.L., Ferreira, T.O., 2022. Short-term Fe reduction and metal dynamics in estuarine soils impacted by Fe-rich mine tailings. Appl Geochem 136, 105134. https://doi.org/10.1016/J.APGEOCHEM.2021.105134.

[11] Cai, Y., Wang, B., Pan, F., Fu, Y., Guo, W., Guo, Z., Liu, H., 2022. Effects of manganese, iron and sulfur geochemistry on arsenic migration in the estuarine sediment of a small river in Xiamen, Southeast China. Environ Pollut 293, 118570. https://doi.org/10.1016/J.ENVPOL.2021.118570.

[12] Saha, A., Vijaykumar, M.E., Das, B.K., Samanta, S., Khan, M.F., Kayal, T., Jana, C., Chowdhury, A.R., 2023. Geochemical distribution and forms of phosphorus in the surface sediment of Netravathi-Gurupur estuary, southwestern coast of India. Mar Pollut Bull 187, 114543. https://doi.org/10.1016/J.MARPOLBUL.2022.114543.

[13] Queiroz, H.M., Nóbrega, G.N., Ferreira, T.O., Almeida, L.S., Romero, T.B., Santaella, S.T., Bernardino, A.F., Otero, X.L., 2018. The Samarco mine tailing disaster: a possible time-bomb for heavy metals contamination? Sci Total Environ 637–638, 498–506. https://doi.org/10.1016/J.SCITOTENV.2018.04.370.

[14] Queiroz, H.M., Ying, S.C., Bernardino, A.F., Barcellos, D., Nóbrega, G.N., Otero, X.L., Ferreira, T.O., 2021. Role of Fe dynamic in release of metals at Rio Doce estuary: unfolding of a mining disaster. Mar Pollut Bull 166, 112267. https://doi.org/10.1016/J.MARPOLBUL.2021.112267.

[15] Queiroz, H.M., Ruiz, F., Deng, Y., de Souza Júnior, V.S., Ferreira, A.D., Otero, X.L., de Lima Camêlo, D., Bernardino, A.F., Ferreira, T.O., 2022. Mine tailings in a redox-active environment: Iron geochemistry and potential environmental consequences. Sci Total Environ 807, 151050. https://doi.org/10.1016/j.scitotenv.2021.151050.

[16] Gomes, L.E. de O., Correa, L.B., Sá, F., Neto, R.R., Bernardino, A.F., 2017. The impacts of the Samarco mine tailing spill on the Rio Doce estuary, Eastern Brazil. Mar Pollut Bull 120, 28–36. https://doi.org/10.1016/J.MARPOLBUL.2017.04.056.

[17] Gabriel, F.Â., Ferreira, A.D., Queiroz, H.M., Vasconcelos, A.L.S., Ferreira, T.O., Bernardino, A.F., 2021. Long-term contamination of the Rio Doce estuary as a result of Brazil's largest environmental disaster. Perspect Ecol Conserv 19, 417–428. https://doi.org/10.1016/J.PECON.2021.09.001.

[18] Hatje, V., Pedreira, R.M.A., de Rezende, C.E., Schettini, C.A.F., de Souza, G.C., Marin, D.C., Hackspacher, P.C., 2017. The environmental impacts of one of the largest tailing dam failures worldwide. Sci Rep 7 (1), 10706. https://doi.org/10.1038/s41598-017-11143-x.

[19] Carmo, F.F. do, Kamino, L.H.Y., Junior, R.T., Campos, I.C. de, Carmo, F.F. do, Silvino, G., Castro, K.J. da S.X. de, Mauro, M.L., Rodrigues, N.U.A., Miranda, M.P. de S., Pinto, C.E.F., 2017. Fundão tailings dam failures: the environment tragedy of the largest technological disaster of Brazilian mining in global context. Perspect Ecol Conserv 15 (3), 145–151. https://doi.org/10.1016/J.PECON.2017.06.002.

[20] Gabriel, F.A., Silva, A.G., Queiroz, H.M., Ferreira, T.O., Hauser-Davis, R.A., Bernardino, A.F., 2020. Ecological risks of metal and metalloid contamination in the Rio Doce Estuary. Integr Environ Assess Manag 16, 655–660. https://doi.org/10.1002/IEAM.4250.

[21] Richard, E. da C., Estrada, G.C.D., Bechtold, J.P., de Aguiar Duarte, H., Maioli, B.G., de Freitas, A.H.A., Warner, K.E., Figueiredo, L.H.M., 2020. Water and Sediment Quality in the Coastal Zone Around the Mouth of Doce River After the Fundão Tailings Dam Failure. Integr Environ Assess Manag 16, 643–654. https://doi.org/10.1002/IEAM.4309.

[22] Longhini, C.M., Rodrigues, S.K., Costa, E.S., da Silva, C.A., Cagnin, R.C., Gripp, M., Lehrback, B.D.C., Mill, G.N., de Oliveira, E.M.C., Hermogenes, C. de C.M., Rodrigues, D.G.F., David, A.M., Gramlich, K.C., Bisi Júnior, R. da C., Gomes, A.A. P., da Silva Filho, J.P., Almeida, J.F., de Souza, K.F., Luz Junior, W.A.R., Poleze, L.M.B., Barros, R.R., Rigo, D., Ghisolfi, R.D., Neto, R.R., Sá, F., 2022. Environmental quality assessment in a marine coastal area impacted by mining tailing using a geochemical multi-index and physical approach. Sci Total Environ 803, 149883. https://doi.org/10.1016/J.SCITOTENV.2021.149883.

[23] Yamamoto, F.Y., Pauly, G.F.E., Nascimento, L.S., Fernandes, G.M., Santos, M.P., Figueira, R.C.L., Cavalcante, R.M., Grassi, M.T., Abessa, D.M.S., 2023. Explaining the persistence of hazardous chemicals in the Doce River (Brazil) by multiple sources of contamination and a major environmental disaster. J Hazard Mater Adv 9, 100250. https://doi.org/10.1016/J.HAZADV.2023.100250.

[24] Alvares, C.A., Stape, J.L., Sentelhas, P.C., De Moraes Gonçalves, J.L., Sparovek, G., 2013. Köppen's climate classification map for Brazil. Meteorol Z 22, 711–728. https://doi.org/10.1127/0941-2948/2013/0507.

[25] Howard, J., Hoyt, S., Isensee, K., Telszewski, M., & Pidgeon, E. (2014). Coastal blue carbon: methods for assessing carbon stocks and emissions factors in mangroves, tidal salt marshes, and seagrasses (1st ed., Vol. 1). International Union for Conservation of Nature. https://cgspace.cgiar.org/handle/10568/95127.

[26] Nóbrega, G.N., Ferreira, T.O., Artur, A.G., de Mendonça, E.S., Leão, de O., R. A., Teixeira, A.S., Otero, X.L., 2015. Evaluation of methods for quantifying organic carbon in mangrove soils from semi-arid region. J Soils Sediment 15, 282–291.

[27] Gee, G.W., Bauder, J.W., 1986. Particle-size Analysis. Methods Soil Anal, Part 1: Phys Mineral Methods 383–411. https://doi.org/10.2136/SSSABOOKSER5.1.2ED.C15.

[28] Otero, X.L., Ferreira, T.O., Vidal-Torrado, P., Macías, F., 2006. Spatial variation in pore water geochemistry in a mangrove system (Pai Matos island, Cananeia-Brazil). Appl Geochem 21, 2171–2186. https://doi.org/10.1016/J.APGEOCHEM.2006.07.012.

[29] Li, S.W., Li, M.Y., Sun, H.J., Li, H.B., Ma, L.Q., 2020. Lead bioavailability in different fractions of mining- and smelting-contaminated soils based on a sequential extraction and mouse kidney model. Environ Pollut 262, 114253. https://doi.org/10.1016/J.ENVPOL.2020.114253.

[30] Ren, J., Williams, P.N., Luo, J., Ma, H., Wang, X., 2015. Sediment metal bioavailability in Lake Taihu, China: evaluation of sequential extraction, DGT, and PBET techniques. Environ Sci Pollut Res 22, 12919–12928. https://doi.org/10.1007/S11356-015-4565-9/METRICS.

[31] USEPA, Method 6010C inductively coupled plasma-atomic emission spectometry, 2 (1997) 1–19. https://www.epa.gov/sites/production/files/2015–07/documents/epa-6010c.pdf (accessed May 3, 2018).

[32] R. Core Team, R, (2021). http://www.r-project.org/index.html (accessed December 28, 2020).
[33] Duarte, E.B., Neves, M.A., de Oliveira, F.B., Martins, M.E., de Oliveira, C.H.R., Burak, D.L., Orlando, M.T.D.A., Rangel, C.V.G.T., 2021. Trace metals in Rio Doce sediments before and after the collapse of the Fundão iron ore tailing dam, Southeastern Brazil. Chemosphere 262, 127879. https://doi.org/10.1016/J.CHEMOSPHERE.2020.127879.
[34] Bronick, C.J., Lal, R., 2005. Soil structure and management: a review. Geoderma 124, 3–22. https://doi.org/10.1016/J.GEODERMA.2004.03.005.
[35] Hersman, L., Maurice, P., Sposito, G., 1996. Iron acquisition from hydrous Fe(III)-oxides by an aerobic Pseudomonas sp. Chem Geol 132, 25–31. https://doi.org/10.1016/S0009-2541(96)00038-1.
[36] Wang, J., Chen, C., 2006. Biosorption of heavy metals by Saccharomyces cerevisiae: A review. Biotechnol Adv 24, 427–451. https://doi.org/10.1016/J.BIOTECHADV.2006.03.001.
[37] Collin, M., Rasmuson, A., 1988. A Comparison of Gas Diffusivity Models for Unsaturated Porous Media. Soil Sci Soc Am J 52, 1559–1565. https://doi.org/10.2136/SSSAJ1988.03615995005200060007X.
[38] Patrick, W.H., Jugsujinda, A., 1992. Sequential Reduction and Oxidation of Inorganic Nitrogen, Manganese, and Iron in Flooded Soil. Soil Sci Soc Am J 56, 1071–1073. https://doi.org/10.2136/SSSAJ1992.03615995005600040011X.
[39] Reiser, R., Stadelmann, V., Weisskopf, P., Grahm, L., Keller, T., 2020. System for quasi-continuous simultaneous measurement of oxygen diffusion rate and redox potential in soil. J Plant Nutr Soil Sci 183, 316–326. https://doi.org/10.1002/JPLN.201900518.
[40] Vepraskas, M.J., Baker, F.G., Bouma, J., 1974. Soil Mottling and Drainage in a Mollic Hapludalf as Related to Suitability for Septic Tank Construction. Soil Sci Soc Am J 38, 497–501. https://doi.org/10.2136/SSSAJ1974.03615995003800030032X.
[41] Zhang, J., Yang, N., Geng, Y., Zhou, J., Lei, J., 2019. Effects of the combined pollution of cadmium, lead and zinc on the phytoextraction efficiency of ryegrass (: Lolium perenne L.). RSC Adv 9, 20603–20611. https://doi.org/10.1039/c9ra01986c.
[42] Karimian, N., Johnston, S.G., Burton, E.D., 2018. Iron and sulfur cycling in acid sulfate soil wetlands under dynamic redox conditions: A review. Chemosphere 197, 803–816. https://doi.org/10.1016/J.CHEMOSPHERE.2018.01.096.
[43] Vives-Peris, V., de Ollas, C., Gómez-Cadenas, A., Pérez-Clemente, R.M., 2019. Root exudates: from plant to rhizosphere and beyond, 39 Plant Cell Rep 2019 39 (1), 3–17. https://doi.org/10.1007/S00299-019-02447-5.
[44] Ferreira, A.D., Queiroz, H.M., Otero, X.L., Barcellos, D., Bernardino, Â.F., Ferreira, T.O., 2022. Iron hazard in an impacted estuary: Contrasting controls of plants and implications to phytoremediation. J Hazard Mater 428, 128216. https://doi.org/10.1016/J.JHAZMAT.2022.128216.
[45] Bauer, I., Kappler, A., 2009. Rates and extent of reduction of Fe(III) compounds and O2 by humic substances. Environ Sci Technol 43, 4902–4908. https://doi.org/10.1021/ES900179S/SUPPL_FILE/ES900179S_SI_001.PDF.
[46] D. Barcellos, C.S. O'connell, W. Silver, C. Meile, A. Thompson, Hot Spots and Hot Moments of Soil Moisture Explain Fluctuations in Iron and Carbon Cycling in a Humid Tropical Forest Soil, Soil Systems 2018, Vol. 2, Page 59. 2 (2018) 59. https://doi.org/10.3390/SOILSYSTEMS2040059.
[47] Chen, C., Meile, C., Wilmoth, J., Barcellos, D., Thompson, A., 2018. Influence of pO2 on Iron Redox Cycling and Anaerobic Organic Carbon Mineralization in a Humid Tropical Forest Soil. Environ Sci Technol 52, 7709–7719. https://doi.org/10.1021/ACS.EST.8B01368/SUPPL_FILE/ES8B01368_SI_001.PDF.
[48] Koch, M.S., Rawlik, P.S., 1993. Transpiration and stomatal conductance of two wetland macrophytes (Cladium jamaicense and Typha domingensis) in the subtropical Everglades. Am J Bot 80, 1146–1154. https://doi.org/10.1002/J.1537-2197.1993.TB15346.X.
[49] Saunders, M.J., Jones, M.B., Kansiime, F., 2007. Carbon and water cycles in tropical papyrus wetlands. Wetl Ecol Manag 15, 489–498. https://doi.org/10.1007/S11273-007-9051-9/METRICS.